Actin-based models of cell migration and chemotaxis

Katherine Broadfoot

Supervisors: Dr John Mackenzie, University of Strathclyde
Professor Robert Insall, Beatson Institute for Cancer Research

27th September, 2013

Contents

1   Abstract

The aim of this paper is to investigate models based mainly on the reaction between filamentous actin and SCAR in *Dictyostelium discoideum*. These reactants play an important role in cell migration, and we expect to observe travelling waves in the model as would be observed in the organism.

Models are constructed from reaction kinetics and analysed for the ability to produce spatial patterns. The model can be constructed to produce a spatial pattern via a Turing instability, however this does not allow for the variation in behaviour that would be expected from a moving cell reacting to signals.

To achieve the level of variability expected in modeling the cell, a three equation system which includes feedback from filamentous actin to activated SCAR was used. It appears that this feedback is necessary to produce the appropriate patterning, such as travelling waves, in the model although the biological reason for this is not yet entirely clear.

2 Introduction

Cell migration plays an important part in the development of most organisms and in processes such as wound healing, immune system response and cancer metastasis [1].

It is generally accepted that cell migration is a complex process mediated by dynamic changes in the actin-myosin cytoskeleton [2].

Constructing models based on the interplay between filamentous actin (F-actin) and its nucleation promoting factors (NPFs), such as SCAR [3] (or WAVE), that activate the actin-related protein Arp2/3 complex should allow better understanding of the dynamics controlling cell migration.

An existing model of interest uses a three equation system, comprising largely of a local activator, global inhibitor and local inhibitor [4]. However, the activator and inhibitors are not described by an exact biological role here. We aim to form models based on a system of biological reactants to elucidate the biology behind this existing model. SCAR exists in three forms: inactive and sensitive, which are cytosolic and active which is membrane-bound. Due to their locations in the cell, the diffusion of active SCAR will be much less than the diffusion of inactive and sensitive.

Models will be based on the observed behaviour of the model organism *Dictyostelium discoideum*, a species of soil-living amoeba. As the cells of this organism move, this is a valuable tool for modelling cell movement.
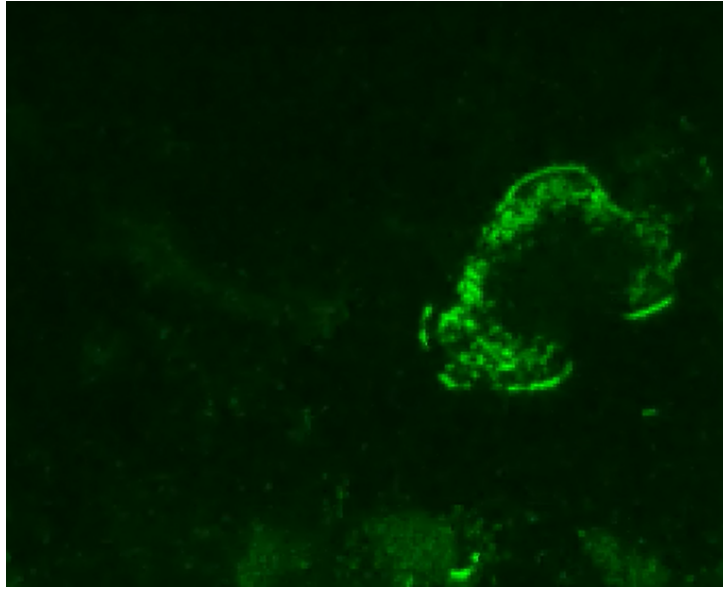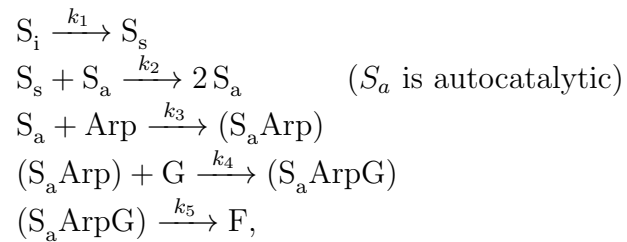
Figure 1: Green flourescent protein (GFP) tagged SCAR waves.[]

Figure 1 shows bright "waves"of actin forming at the leading edge of the moving cell. This, in particular, is what we aim to model and we should observe waves in filamentous actin and its NPFs such as SCAR that could represent a system such as this, with enough variability to respond to extracellular signalling (such as chemoattractants/repellents).

3 Model From Reaction Kinetics

A reaction system describing the kinetics of F-actin and its NPFs was created based on experimental observations:

$$
\begin{aligned}
&\mathrm{S_i} \xrightarrow{k_1} \mathrm{S_s} \\
&\mathrm{S_s} + \mathrm{S_a} \xrightarrow{k_2} 2\,\mathrm{S_a} \qquad (S_a \text{ is autocatalytic}) \\
&\mathrm{S_a} + \mathrm{Arp} \xrightarrow{k_3} (\mathrm{S_a Arp}) \\
&(\mathrm{S_a Arp}) + \mathrm{G} \xrightarrow{k_4} (\mathrm{S_a ArpG}) \\
&(\mathrm{S_a ArpG}) \xrightarrow{k_5} \mathrm{F},
\end{aligned}
$$

where S_i, S_s and S_a represent inactive, sensitive and active SCAR respectively and Arp, G and F represent Arp2/3, globular actin and filamentous actin. In addition $k_1, \ldots, k_5$ are the reaction rates, $S_a Arp$ is the complex formed by the binding of S_a and Arp and $S_a ArpG$ is the complex formed by the binding of S_a, Arp and G.

By assuming that the law of mass action holds, that $[S_i], [Arp]$ and $[G]$ ($[\ ]$ is used to denote the concentration of the reactants) are sufficiently abundant to allow them to be considered constant and that F-actin is additionally depleted linearly, we arrive at the following system of ordinary differential equations (ODEs):

$$
\begin{aligned}
\frac{d[S_s]}{dt} &= k_1[S_i] - k_2[S_s][S_a] \\
\frac{d[S_a]}{dt} &= k_2[S_s][S_a] - k_3[S_a][Arp] \\
\frac{d[S_a Arp]}{dt} &= k_3[S_a][Arp] - k_4[S_a Arp][G] \\
\frac{d[S_a ArpG]}{dt} &= k_4[S_a Arp][G] - k_5[S_a ArpG] \\
\frac{d[F]}{dt} &= k_5[S_a ArpG] - k_6[F].
\end{aligned}
\tag{1}
$$

These equations describe a situation where the variables are constant in space (a well-mixed system). The system's steady state occurs when the derivatives are zero.

$$
\begin{aligned}
\frac{d[S_s]}{dt} &= k_1[S_i] - k_2[S_s][S_a] = 0 \Rightarrow [S_s][S_a] = \frac{k_1[S_i]}{k_2} \\
\frac{d[S_a]}{dt} &= k_2[S_s][S_a] - k_3[S_a][Arp] = 0 \Rightarrow [S_a] = \frac{k_2[S_s][S_a]}{k_3[Arp]} = \frac{k_1[S_i]}{k_3} \\
\frac{d[S_aArp]}{dt} &= k_3[S_a][Arp] - k_4[S_aArp][G] = 0 \Rightarrow [S_aArp] = \frac{k_3[S_a][Arp]}{k_4[G]} = \frac{k_1[S_i][Arp]}{k_4[G]} \\
\frac{d[S_aArpG]}{dt} &= k_4[S_aArp][G] - k_5[S_aArpG] = 0 \Rightarrow [S_aArpG] = \frac{k_4[S_aArp][G]}{k_5} = \frac{k_1[S_i][Arp]}{k_5} \\
\frac{d[F]}{dt} &= k_5[S_aArpG] - k_6[F] = 0 \Rightarrow [F] = \frac{k_5[S_aArpG]}{k_6} = \frac{k_1[S_i][Arp]}{k_6}
\end{aligned}
$$

Therefore the steady state is unique in terms of the parameters.

$$
\begin{aligned}
[S_s] &= \frac{k_3}{k_2} \\
[S_a] &= \frac{k_1[S_i]}{k_3} \\
[S_aArp] &= \frac{k_1[S_i][Arp]}{k_4[G]} \\
[S_aArpG] &= \frac{k_1[S_i][Arp]}{k_5} \\
[F] &= \frac{k_1[S_i][Arp]}{k_6}
\end{aligned}
$$

The stability of steady states can be analysed by considering the eigenvalues of the Jacobian matrix of the system evaluated at the steady state. As the eigenvalues of the Jacobian all have negative real parts, the steady state is always stable. However, the parameters can be chosen so that the solution returns to the steady state via oscillations, as shown below.
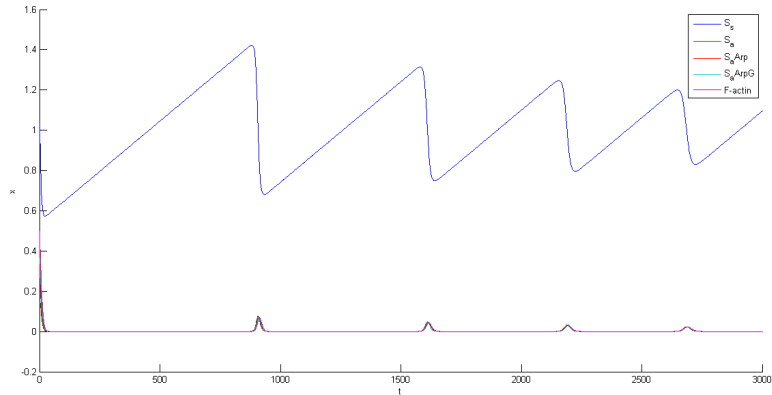
Figure 2: Perturbation leads to oscillations in sensitive SCAR, which is followed by oscillations in the other variables including F-actin.

The observations in Figure 2 match the expected biological behaviour quite closely as sensitive SCAR produces the active form of SCAR and this will build up and lead to a burst of filamentous actin. After this burst, the activated form is depleted until sensitive builds up again and continues in this process, creating the oscillations. However, the waves in the biological system would not be expected to die away to a steady state. Cells would continue to react to signals, changing their behaviour in response to signals and creating waves in SCAR and actin as the move.

Additionally, the biological system would include diffusion across the cell of the reactants. To improve the model, diffusion in one dimension was added. This gives

$$\frac{\partial [S_s]}{\partial t} = k_1[S_i] - k_2[S_s][S_a] + D_s\nabla^2[S_s]$$

$$\frac{\partial [S_a]}{\partial t} = k_2[S_s][S_a] - k_3[S_a][Arp] + D_a\nabla^2[S_a]$$

$$\frac{\partial [S_aArp]}{\partial t} = k_3[S_a][Arp] - k_4[S_aArp][G] + D_3\nabla^2[S_aArp] \qquad (2)$$

$$\frac{\partial [S_aArpG]}{\partial t} = k_4[S_aArp][G] - k_5[S_aArpG] + D_4\nabla^2[S_aArpG]$$

$$\frac{\partial [F]}{\partial t} = k_5[S_aArpG] - k_6[F] + D_F\nabla^2[F].$$

Where $D_s, \ldots, D_F$ are the diffusion coefficients of the appropriate variable. However, this system does not appear to produce any spatial patterns. To analyse the possibility of spatial patterns arising from this model, the system is simplified.

4 Two Equation Model

By assuming $[S_aArp]$ and $[S_aArpG]$ are approximately steady (i.e. $\frac{d[S_aArp]}{dt} \approx \frac{d[S_aArpG]}{dt} \approx 0$) and then combining constants, the model can be simplified to

$$\frac{d[S_s]}{dt} = k_1[S_i] - k_2[S_s][S_a] = c_1 - c_2[S_s][S_a] \qquad (3)$$

$$\frac{d[S_a]}{dt} = k_2[S_s][S_a] - k_3[S_a][Arp] = c_2[S_s][S_a] - c_3[S_a] \qquad (4)$$

$$\frac{d[F]}{dt} = c_3[S_a] - c_4[F] \qquad (5)$$

Where $c_1 = k_1[S_i]$, $c_2 = k_2$ and $c_3 = k_3[Arp]$. Similarly, $\frac{d[S_aArp]}{dt} \approx \frac{d[S_aArpG]}{dt} \approx 0 \Rightarrow k_5[S_aArpG] \approx k_4[S_aArp][G] \approx k_3[S_a][Arp] = c_3[S_a]$.

As there is no feedback from equation (6) onto equations (4) and (5), it decouples from the other equations, leaving a system comprising equations (4)

and (5).

The system behaves similarly to the full system; the steady state is stable, and parameters can be chosen to give oscillations when returning to steady state from a perturbation.

Adding in diffusion as before gives the following system of PDEs:

$$\frac{\partial [S_s]}{\partial t} = c_1 - c_2[S_s][S_a] + D_s\nabla^2[S_s] := f_1([S_s],[S_a]) + D_s\nabla^2[S_s] \qquad (6)$$

$$\frac{\partial [S_a]}{\partial t} = c_2[S_s][S_a] - c_3[S_a] + D_a\nabla^2[S_a] := f_2([S_s],[S_a]) + D_a\nabla^2[S_a]. \, (7)$$

To analyse the potential for spatial patterns in this system, Turing pattern analysis is used [5]. However, with $d = \frac{D_a}{D_s}$, one of the necessary conditions $(d\frac{\partial f_1}{\partial [S_s]} + \frac{\partial f_2}{\partial [S_a]} > 0)$ for a spatial pattern arising via Turing instability is not satisfied as $d\frac{\partial f_1}{\partial [S_s]} = -dc_2[S_a] < 0$ and $\frac{\partial f_2}{\partial [S_a]} = 0$, $d = \frac{D_a}{D_s}$, so d must be positive. Therefore this system cannot give rise to spatial patterns via a Turing instability, as was expected since the system of five equations did not appear to produce this type of pattern.

To allow for the possibility of spatial patterns via Turing instability, the autocatalytic terms were altered so that

$$\frac{\partial [S_s]}{\partial t} = c_1 - c_2[S_s]^2[S_a] + D_s\nabla^2[S_s] := f_1 + D_s\nabla^2[S_s] \qquad (8)$$

$$\frac{\partial [S_a]}{\partial t} = c_2[S_s]^2[S_a] - c_3[S_a] + D_a\nabla^2[S_a] := f_2 + D_a\nabla^2[S_a]. \qquad (9)$$

Again, many of the five equation model's features are preserved. By considering the corresponding ODEs, it is clear that a unique steady state, dependent on the values of the parameters, exists.

$$\begin{aligned}
\frac{d[S_s]}{dt} &= c_1 - c_2[S_s][S_a]^2 = 0, \\
\frac{d[S_a]}{dt} &= c_2[S_s][S_a]^2 - c_3[S_a] = 0 \\
\Rightarrow [S_a] &= \frac{c_1}{c_3}, \\
[S_s] &= \frac{c_3^2}{c_1 c_2}
\end{aligned}$$

However, the parameters can now be chosen so that spatial patterns can arise from a Turing instability. This requires that the following necessary conditions are satisfied

$$\frac{\partial f_1}{\partial [S_s]} + \frac{\partial f_2}{\partial [S_a]} < 0 \tag{10}$$

$$\frac{\partial f_1}{\partial [S_s]}\frac{\partial f_2}{\partial [S_a]} - \frac{\partial f_1}{\partial [S_a]}\frac{\partial f_2}{\partial [S_s]} > 0 \tag{11}$$

$$d\frac{\partial f_1}{\partial [S_s]} + \frac{\partial f_2}{\partial [S_a]} > 0 \tag{12}$$

$$\left(\frac{\partial f_1}{\partial [S_s]} + \frac{\partial f_2}{\partial [S_a]}\right)^2 - 4d\left(\frac{\partial f_1}{\partial [S_s]}\frac{\partial f_2}{\partial [S_a]} - \frac{\partial f_1}{\partial [S_a]}\frac{\partial f_2}{\partial [S_s]}\right) > 0. \tag{13}$$

One of the requirements this imposes is $d = \frac{D_a}{D_s} < 1 \Rightarrow D_a < D_s$ as well as restricting the choices of c_1, c_2 and c_3. This requirement can be biologically justified as sensitive SCAR resides in the cystolic area of the cell, whereas active SCAR is mostly membrane bound. The diffusion in the membrane is slower than in the cystol, so it would follow that the diffusion coefficient of active SCAR will be less than that of sensitive SCAR ($D_a < D_s$).

Although this does produce spatial patterning, Turing patterns are very stable, as seen in figures 3 and 4. A cell would respond to extracellular stimuli which would produce variations in the patterns, which will not be observed with Turing patterns.
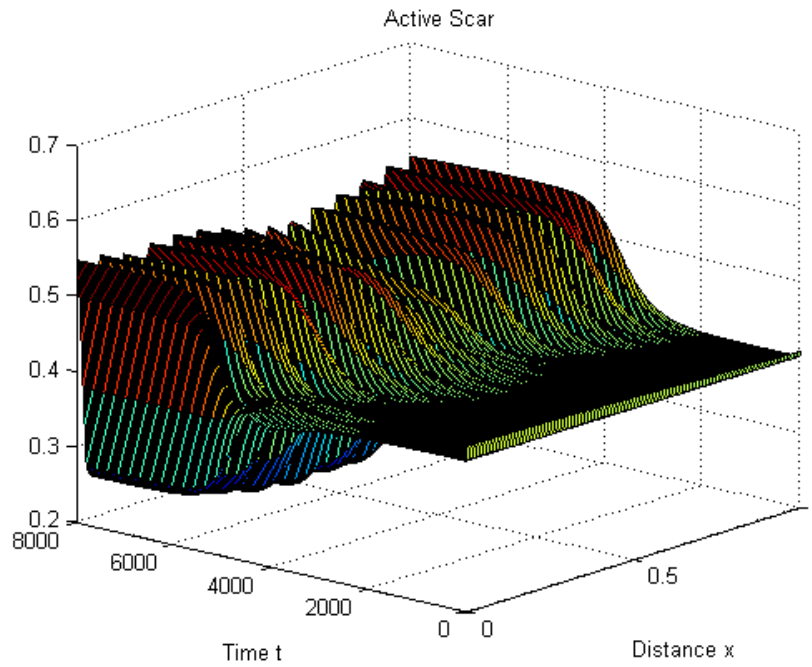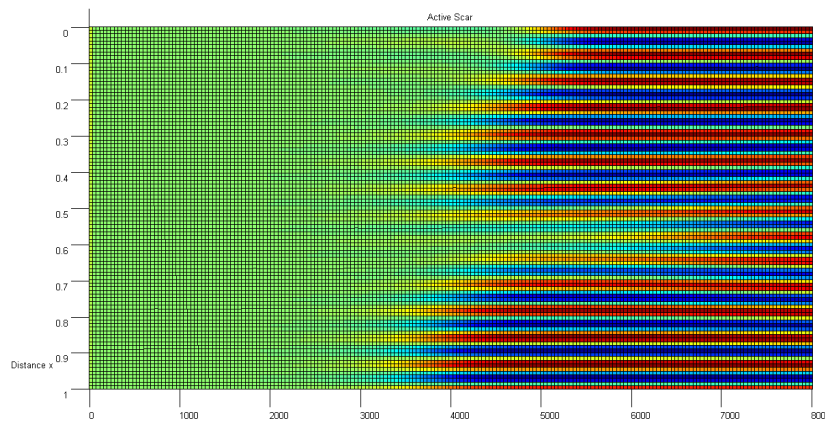
Figure 3: A spatial pattern is set up.

Figure 4: Once the pattern is set up it is very stable.

5 Three Equation Model

To produce the variability in spatial patterns that would be expected from
the biological system, a similar approach to that taken in the literature[6, 7, 8]

was used, so that the system is described by

$$\frac{\partial[S_s]}{\partial t} = c_1 - \frac{c_2[S_s]([S_a]^2 + c_3)}{[F](1 + c_4[S_a]^2)} + D_s\nabla^2[S_s] \tag{14}$$

$$\frac{\partial[S_a]}{\partial t} = \frac{c_2[S_s]([S_a]^2 + c_3)}{[F](1 + c_4[S_a]^2)} - c_5[S_a] + D_a\nabla^2[S_a] \tag{15}$$

$$\frac{\partial[F]}{\partial t} = c_6([S_a] - [F]) + D_F\nabla^2[F] \tag{16}$$

This system includes feedback from filamentous actin on SCAR. The model without diffusion of ordinary differential equations for this system has limit cycle kinetics, so will not return to a steady state.

The model produces spatial patterns which are not stable, they will change over time. The pattern begins in a stable fashion, then out of phase oscillations start to form before becoming travelling waves.
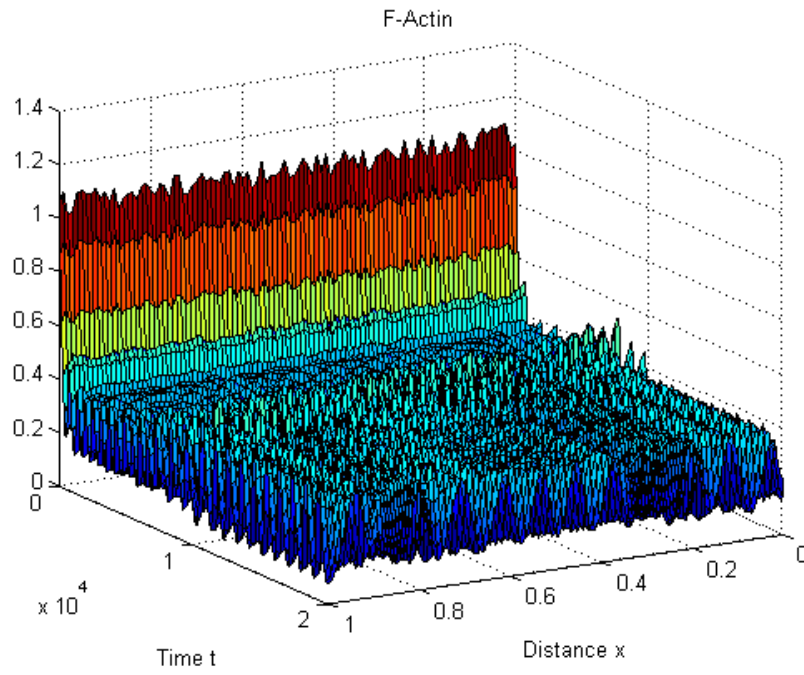
Figure 5: The spatial patterns represent a more realistic system, with a greater ability to change in response to stimulants.
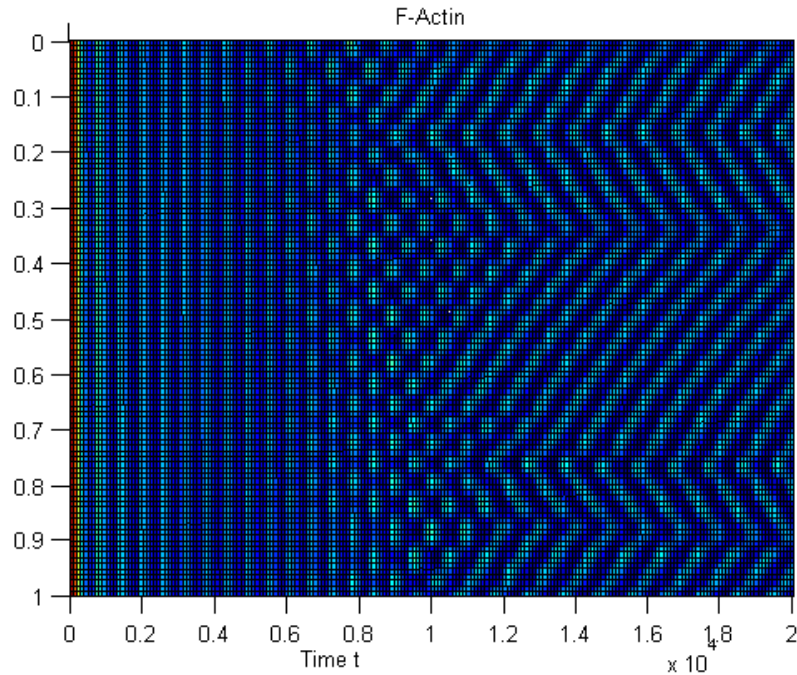
Figure 6: The stable spatial pattern becomes out of phase oscillations and then travelling waves.

6 Conclusions

Although the two equation model allowed spatial patterns to form via Turing instability, these patterns are very stable and are more often used to describe patterns on animals (e.g. a Zebra's stripes or a Leopard's spots) which will not change once they have been formed. For the model to accurately describe the system we are modelling, a less stable pattern is required.

The need for the type of three equations system that has been used would imply that filamentous actin must negatively regulate active SCAR. There is no obvious biological reason for this to be true, although possible reasons have been suggested that F-actin encourages active SCAR to come off the membrane, causing feedback [9], but the biological evidence supporting this would benefit from closer investigation.

Future work on this project could include the inclusion of diffusion in two

14

dimensions, and solving the differential equations on a moving boundary (representing the membrane of the cell). This would better represent the biological system and improve the accuracy of the model.

7 References

[1] Lauffenberger, D.A. & Horwitz, A.F. (1996) Cell Migration: A Physically Integrated Molecular Process. *Cell.* **9**(3), 359–369.

[2] Cooper, G.M. The Cell: A Molecular Approach. 2nd edition. Sunderland (MA): Sinauer Associates; 2000. Actin, Myosin, and Cell Movement. Available from: http://www.ncbi.nlm.nih.gov/books/NBK9961/

[3] Pollitt, A.Y., Insall, R.H.(2009). WASP and SCAR/WAVE proteins: the drivers of actin assembly. *J Cell Sci.* **122**, 2575–2578.

[4] Neilson, M.P., Veltman, D.M., van Hastert, P.J.M., Webb, S.D., Mackenzie, J.A., et al. (2011) Chemotaxis: A Feedback-Based Computational Model Robustly Predicts Aspects of Real Cell Behaviour. *PLoS Biol.* **9** (5): e1000618. doi:10.137/journal.pbio.1000618

[5] Murray, J.D. (1989) Mathematical Biology (2nd Ed) Berlin: Springer-Verlag

[6] Meinhardt,H. (2004) Out-of-phase oscillations and traveling waves with unusual properties: the use of three-component systems in biology, *Physica D: Nonlinear Phenomena.* **199**(1-2), 264–277.

[7] Holmes, W.R., Carlsson, A.E. & Edelstein-Keshet, L. (2012) Regimes of Wave Type Patterning Driven by Refractory Actin Feedback: Transition from Static Polarization to Dynamic Wave Behaviour. *Phys. Biology.* **9** (4), 046005.

[8] Carlsson, A.E. (2010) Dendritic Actin Filament Nucleation Causes Traveling Waves and Patches. *Phys Rev Lett.* **104**:228102

[9] Weiner, O.D., Margansk, W.A., Wu, L.F., Altschuler, S.J., Kirschner, M.W. (2007) An Actin-Based Wave Generator Organizes Cell Motility. *PLoS Biol* **5**(9): e221. doi:10.1371/journal.pbio.0050221